

Article

Ultimate Bearing Capacity of Bottom Sealing Concrete in Underwater Deep Foundation Pit: Theoretical Calculation and Numerical Analysis

Shuo Chen ¹, Yonghai Li ², Panpan Guo ^{1,*} , Xiaohan Zuo ¹, Yan Liu ³, Haiping Yuan ¹  and Yixian Wang ^{1,3,*} ¹ School of Civil Engineering, Hefei University of Technology, Hefei 230009, China² The Second Engineering Co., Ltd. of CTCE Group, Suzhou 215131, China³ State Key Laboratory of Explosion Science and Technology, Beijing Institute of Technology, Beijing 100081, China

* Correspondence: pp_guo@zju.edu.cn (P.G.); wangyixian2012@hfut.edu.cn (Y.W.)

Abstract: The cofferdam method is generally applied in the construction of underwater pier foundation in bridge engineering, and the pouring of bottom sealing concrete is one of the important links in the construction of the cofferdam. The bottom sealing concrete can prevent water seepage and balance the main body of the cofferdam, and its structural size and construction quality have a great influence on the above functions. Under the condition of large water level difference, it is difficult to determine the reasonable thickness of the bottom sealing concrete. There are few related studies in this field, and there is a lack of systematic summary of calculation theory. This work theoretically deduces the approximate solution of ultimate bending moment and ultimate stress of the bottom sealing concrete, introduces two different calculation methods, systematically summarizes the calculation methods of three kinds of ultimate stress, analyzes the calculation methods of ultimate bonding force, and uses ANSYS finite element software to simulate a specific bottom sealing concrete model, and compares it with the theoretical calculation results. The maximum stress obtained by the approximate solution is closer to the actual monitoring data than the traditional method, and the calculation method of the bonding force can be used to make a rough estimate.

Keywords: deep-water foundation; cofferdam; bottom sealing concrete; ultimate bearing capacity; elasticity; numerical simulation



Citation: Chen, S.; Li, Y.; Guo, P.; Zuo, X.; Liu, Y.; Yuan, H.; Wang, Y.

Ultimate Bearing Capacity of Bottom Sealing Concrete in Underwater Deep Foundation Pit: Theoretical Calculation and Numerical Analysis. *Machines* **2022**, *10*, 830. <https://doi.org/10.3390/machines10100830>

Academic Editor: Valter Carvelli

Received: 15 August 2022

Accepted: 15 September 2022

Published: 21 September 2022

Publisher's Note: MDPI stays neutral with regard to jurisdictional claims in published maps and institutional affiliations.



Copyright: © 2022 by the authors. Licensee MDPI, Basel, Switzerland. This article is an open access article distributed under the terms and conditions of the Creative Commons Attribution (CC BY) license (<https://creativecommons.org/licenses/by/4.0/>).

1. Introduction

Bridges across rivers and seas all need to build deep-water foundations, which have become a critical part in the construction of large-span bridges due to their difficult construction, high safety risks and long construction period [1,2]. In recent years, the large-scale pile group foundation widely used in the deep-water foundations of bridges in China is the development trend of deep-water foundations of bridges, and various cofferdam construction technologies have developed accordingly. General forms of cofferdam mainly include steel sheet pile cofferdam, concrete cofferdam, steel boxed cofferdam, steel hoisting box cofferdam, steel-concrete combined cofferdam, etc. [3].

The cofferdam used in the construction of deep-water bridges is not only the construction platform for the bored piles in the early stage, but also the water-retaining structure for the construction of the later stage caps. It has always been the focus and difficulty in the construction. In the cofferdam foundation construction, after pouring the bottom sealing concrete, the cofferdam should be pumped to form a dry environment for the construction of the cap. At this time, the bottom of the cofferdam mainly resists the huge buoyancy through the adhesion between the bottom sealing concrete and the steel pipe pile (surrounded externally by the steel sleeves).

Scholars have conducted extensive theoretical and applied research on various cofferdams (particularly steel sheet pile cofferdams), mainly including cofferdam structure calculation, seepage and construction plan design.

Blum [4] firstly studied the problem of bending stiffness reduction of steel sheet piles; Lohmeyer [5] studied the bending strength of steel sheet pile walls and proposed a numerical model that can evaluate the shear failure caused by slip between piles. The influence of the bending stiffness is fully transmitted. Terzaghi [6] studied the stability and stiffness of cellular cofferdams. After that, Ovesen [7] also studied the cellular cofferdam. Sunir Mal Banerjee [8] drew the design chart of the double-walled cofferdam and summarized the construction method of the double-walled cofferdam. Dr.-Ing. Hans-Dieter Clasmeier [9] pointed out that modern cofferdams may have evolved from steel sheet piles in the early 20th century. During construction, the steel sheet piles driven into the water are horizontally connected and locked to form a modern cofferdam with higher strength. Lefas et al. [10] established a simplified two-dimensional model to analyze the structure of steel sheet pile cofferdams and analyzed the force and deformation characteristics of the cofferdam during the construction process by writing a program and demonstrated the rationality of this model by comparing with traditional methods. Hu [11] studied the application and development of construction technology of double-walled steel cofferdam for bridge foundations. Pan et al. [12] studied the deformation and internal force characteristics of steel sheet pile cofferdams under different construction procedures. Li [13] conducted research on water-stop performance test and structural design of steel sheet pile cofferdam. Wen [14] used the method of model test to study the value of the bonding force between the sealing concrete of the double-walled steel cofferdam and the steel protective tube. Chen [15] conducted researches on the anti-floating characteristics of deep foundation pit concrete sealing structure. He [16] studied the construction technology of the steel cofferdam in complicated hydro-geological conditions. Hua [17] analyzed the mechanical behavior of double wall steel cofferdam by monitoring the stress. Yu [18] analyzed the mechanical characteristics of the single wall steel cofferdam in deep water construction and researched the key technology. In addition, Divyah N. [19], Rafael Alves de Souza [20], Vinay Shimpi [21] and other scholars [22–27] also did some relevant researches on the cofferdams.

At present, there are few studies on the ultimate bearing capacity of the bottom sealing concrete of the underwater deep foundation pit engineering, and there is no systematic calculation theory summary about this, which is not enough to guide the construction of such projects. Therefore, it is necessary to conduct a systematic study on the calculation theory of the ultimate bearing capacity of the bottom sealing concrete to provide a reference for similar projects.

Besides, traditional empirical data is mostly used for the value of the bonding stress between the concrete and the steel pipe pile at the bottom of the cap. There are very few studies on this, the test results of various units are quite different, the test data is also less, the versatility is poor, and it is not enough to guide the construction of various bridges. In addition, the influence of the ratio of concrete thickness to steel pipe pile diameter and concrete strength grade on the bonding stress remains to be studied.

2. Theoretical Calculation

As shown in Figure 1, there is the simplified model of the bottom sealing concrete of an underwater deep foundation pit project. The model has a length of a , a width of b , and a thickness of d ($a > b \gg d$). There are several cylindrical holes in the middle (the contact surface with the steel sleeves), and the four sides of the bottom sealing concrete are in contact with the cofferdam.

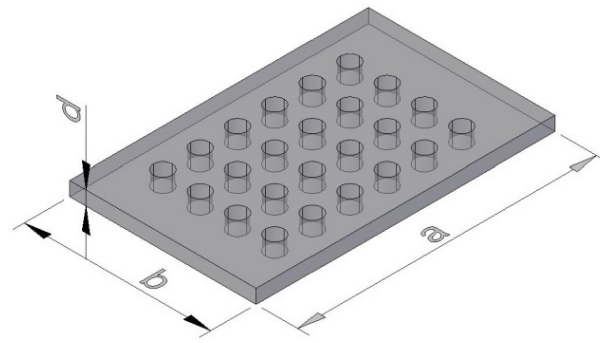


Figure 1. Bottom sealing concrete model diagram.

The forces acting on the bottom sealing concrete are as follows: the vertical downward self-weight G , the vertical upward cohesive force f (acting on the contact surface between the bottom sealing concrete and the cofferdam, and the contact surface between the bottom sealing concrete and the steel sleeves) and the vertical upward buoyancy F (acting on the bottom surface of the bottom sealing concrete). Under the combined action, the bottom sealing concrete is in static equilibrium. The area of the bottom surface of the bottom sealing concrete is A , and the area of the contact surface with the steel sleeves is B . The maximum bending moment that the bottom sealing concrete can withstand needs to be solved to determine its maximum compressive stress and tensile stress. At the same time, the bonding force between the bottom sealing concrete and the steel sleeves also needs to be solved.

2.1. Ultimate Bending Moment and Ultimate Stress

For the calculation of the ultimate bending moment and ultimate stress of the bottom sealing concrete, this article lists two calculation methods.

2.1.1. Approximate Solution Derived by Elasticity Method

The length and width of the bottom sealing concrete are generally much larger than its thickness. At the same time, the bottom sealing concrete can be regarded as an isotropic, continuous, uniform, and small deformation elastic material, whose elastic modulus is E and Poisson's ratio is μ , thus simplifying the bottom sealing concrete. It is an elastic thin slab, which is solved by using elasticity method.

Consider the simplest case. As shown in Figure 2, a certain underwater deep foundation pit project is only equipped with one steel sleeve, and the bottom sealing concrete has only one cylindrical hole. Fill up the cylindrical holes, and treat the bottom sealing concrete as a complete rectangular elastic thin slab simply supported on four sides. This thin slab is subjected to a uniformly distributed load acting on the bottom surface in the vertical upward direction and its strength is q . There is the following equation to calculate q :

$$q = \frac{F - G}{A} \quad (1)$$

Compared with the thin slab with one hole, the completed thin slab lacks the frictional resistance at the contact surface with the steel sleeve, which is equivalent to lack of one support. Besides, the completed thin slab has a uniformly distributed load on the effective area. With the load increasing, the internal stress will also increase. Therefore, for the thin slab with holes, its maximum stress will not exceed the maximum stress of the completed thin slab. Therefore, the maximum stress of the completed slab is used as the maximum stress of the bottom sealing concrete, which makes the calculation result safer.

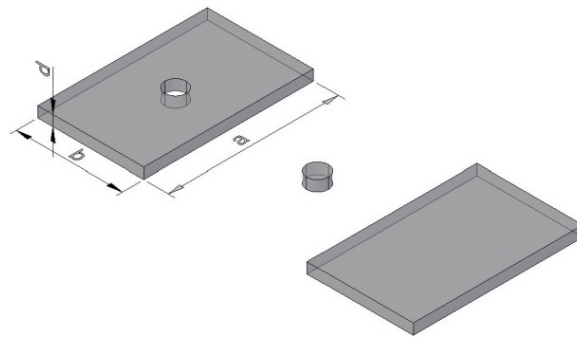


Figure 2. Modified bottom sealing concrete model diagram.

For the completed thin slab, by the Levy solution of a simply supported rectangular thin slab on four sides [28,29], the bending moment at the center of the thin slab is the largest, and the maximum bending moment along the long side is:

$$M_x = \beta_x qa^2 \quad (2)$$

$$\beta_x = \frac{1}{8} - \frac{2}{\pi^3} \sum_{m=1,3,5,\dots}^{\infty} \frac{(-1)^{\frac{m-1}{2}} [(1-\mu)a_m tha_m + 2]}{m^3 cha_m} \quad (3)$$

among them:

$$a_m = \frac{m\pi b}{2a} \quad (4)$$

$$tha_m = \frac{e^{a_m} + e^{-a_m}}{e^{a_m} - e^{-a_m}} \quad (5)$$

$$cha_m = \frac{e^{a_m} + e^{-a_m}}{2} \quad (6)$$

Maximum bending moment along the short side is:

$$M_y = \beta_y qa^2 \quad (7)$$

$$\beta_y = \frac{\mu}{8} + \frac{2}{\pi^3} \sum_{m=1,3,5,\dots}^{\infty} \frac{(-1)^{\frac{m-1}{2}} [(1-\mu)a_m tha_m - 2\mu]}{m^3 cha_m} \quad (8)$$

Maximum compressive stress along the long side is:

$$\sigma_{cx} = -\frac{6M_x}{d^2} = -\frac{6\beta_x qa^2}{d^2} \quad (9)$$

Maximum compressive stress along the short side is:

$$\sigma_{cy} = -\frac{6M_y}{d^2} = -\frac{6\beta_y qa^2}{d^2} \quad (10)$$

Maximum tensile stress along the long side is:

$$\sigma_{tx} = \frac{6M_x}{d^2} = \frac{6\beta_x qa^2}{d^2} \quad (11)$$

Maximum tensile stress along the short side is:

$$\sigma_{ty} = \frac{6M_y}{d^2} = \frac{6\beta_y qa^2}{d^2} \quad (12)$$

where M_x = The maximum bending moment along the long side; β_x = The coefficient for calculating M_x ; a_m = The parameter for calculating β_x ; m = The parameter that determines the calculation accuracy, and only odd numbers are taken; e = Natural constant; π = Ratio of circumference to diameter; μ = Poisson's ratio; q = Strength of distributed load; a = Length

of the bottom sealing concrete; d = Thickness of the bottom sealing concrete; M_y = The maximum bending moment along the short side; β_y = The coefficient for calculating M_y ; σ_{cx} = Maximum compressive stress along the long side; σ_{cy} = Maximum compressive stress along the short side; σ_{tx} = Maximum tensile stress along the long side; σ_{ty} = Maximum tensile stress along the short side.

Analyzing the above equations, it can be found that the convergence speed of σ_{cx} , σ_{cy} , σ_{tx} and σ_{ty} is faster. For actual projects, different convergence terms can be selected according to accuracy requirements.

2.1.2. Traditional Method

According to the traditional method, the strength of the bottom sealing concrete needs to be checked by the following formula:

$$d = \sqrt{\frac{9.09M_{max}}{b_0\sigma_t}} \quad (13)$$

where d = Minimum thickness of the bottom sealing concrete; M_{max} = The standard value of the maximum bending moment per meter width of the bottom sealing concrete; b_0 = Unit width, the value is 1 m; σ_t = The design value of concrete tensile strength.

For the calculation method of the maximum bending moment per meter width of the bottom sealing concrete, as shown in Figure 3, the bottom sealing concrete thin slab can be divided along the long side direction, divided into several concrete beams with fixed supports at both ends, and the bottom bears uniform load. The concrete beam with a rectangular cross-section of unit width (that is, the width of the beam is 1 m) is used for analysis and calculation, as shown in Figure 4.

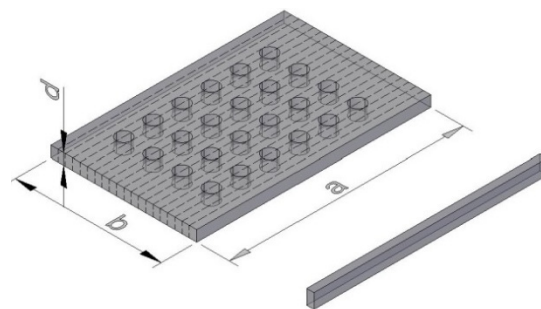


Figure 3. Divided bottom sealing concrete model diagram.

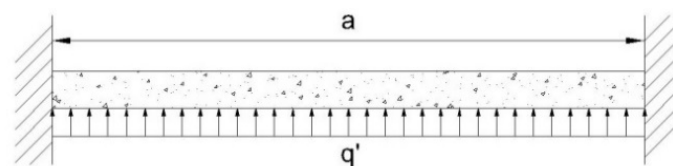


Figure 4. Schematic diagram of concrete beam calculation.

According to this calculation method, the force between adjacent concrete beams is not considered, which will make the calculation result of bending moment larger. Take the concrete beam with the largest span for calculation and analysis, that is, take the concrete beam with the long side length a of the span, which is the most dangerous concrete beam.

Suppose b_0 is the unit width (that is, $b_0 = 1$ m), the uniform load strength is $q' = qb_0$, and the maximum bending moment can be obtained as:

$$M_{max} = \frac{q'a^2}{12} = \frac{qb_0a^2}{12} \quad (14)$$

Substituting Equation (13) to get the minimum thickness of the bottom sealing concrete is:

$$d = \sqrt{\frac{9.09qa^2}{12\sigma_t}} \quad (15)$$

The maximum tensile stress of the bottom sealing concrete is:

$$\sigma_t = \frac{9.09qa^2}{12d^2} \quad (16)$$

2.2. Ultimate Bonding Strength

When calculating the bonding force, ignoring the force between the bottom sealing concrete and the cofferdam. In fact, the bottom sealing concrete is in static equilibrium under the combined action of gravity, buoyancy and friction (including the friction exerted by the cofferdam and the steel sleeves). However, due to the different types of cofferdams and materials used, the friction between cofferdam and concrete is usually difficult to determine. For example, for the steel sheet pile cofferdam, lubricant will be added between adjacent steel sheet piles during construction, and the friction between steel sheet piles and concrete will be reduced due to the presence of lubricant. In this case, the friction between the steel sleeves and the concrete should be focused first.

The bonding force acts on the contact surface between the cylindrical holes of the bottom sealing concrete and the steel sleeves, and the total area of the contact surface is B . The force analysis of the bottom sealing concrete shows that it is balanced under the action of the vertical downward self-weight G , the vertical upward buoyancy F , and the vertical downward cohesive force f . Assuming that the bonding force is evenly distributed on the acting surface and the calculated bonding force is only the average value, then:

$$f = F - G = pA \quad (17)$$

$$\tau = \frac{f}{B} = \frac{pA}{B} \quad (18)$$

For the ultimate bonding force between the bottom sealing concrete and the steel sleeves, according to engineering experience, it is initially taken as 150 kPa. Therefore, as long as $\tau \leq 150$ kPa, the strength requirement can be met [14].

3. Numerical Simulation and Theoretical Verification Calculation

3.1. Numerical Simulation Based on ANSYS

The submerged foundation of Pier 51 of the Ziyang Hanjiang River Bridge is a deep-water foundation of piles [30]. The foundation consists of many rock-socketed piles. The project uses a steel hoisting box cofferdam. The relevant parameters of the engineering are shown in Table 1. The layout of the steel sleeves is shown in Figures 5 and 6.

Table 1. Relevant parameters of the engineering case.

Parameters	Values
Piles' Length	49.0 m
Piles' Diameter	2.0 m
Piles' Number	24
Cofferdam's Long	27.5 m
Cofferdam's Wide	19.2 m
Thickness of the Bottom Sealing Concrete	3.0 m

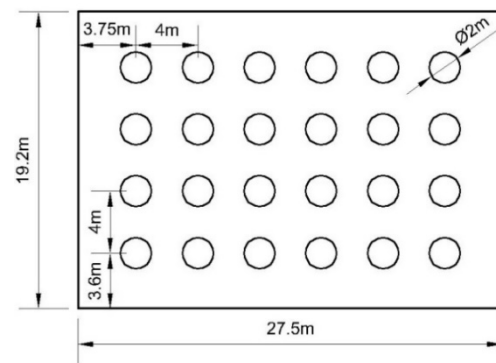


Figure 5. Top view of the bottom sealing concrete of the project.

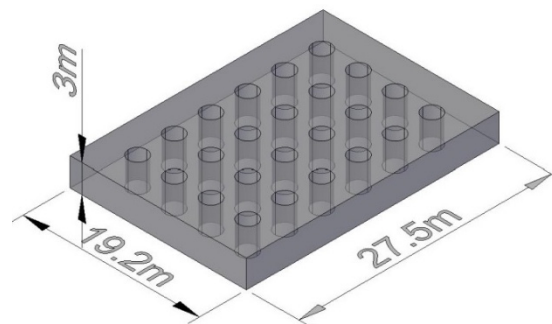


Figure 6. Bottom sealing concrete model diagram of the project.

ANSYS software is used to simulate the bearing status of the bottom sealing concrete. The element type is selected as the concrete65 element. The finite element model adopts quadrilateral meshing. The maximum element side length is 0.5 m. The elastic modulus of the concrete material is set to $E = 28 \text{ GPa}$, and the Poisson’s ratio is $\mu = 0.2$. The boundary conditions of the bottom sealing concrete are fixed on all sides, and the hole in the middle in contact with the steel protective tube restricts the vertical displacement. The model assumes that the bottom sealing concrete material is isotropic, homogeneous, and dense.

Calculation conditions: The bottom sealing concrete is affected by its own weight and buoyancy, the design thickness is 3.0 m, the plain concrete weight is 24 kN/m^3 , and the combined force of its own weight and head buoyancy is applied at 89.57 kPa from the bottom of bottom sealing concrete according to the uniformly distributed load on the surface. Suppose the long side direction is the x -axis, the short side direction is the y -axis, and the thickness direction is the z -axis, the normal stress cloud diagram of the bottom sealing concrete along the x -axis direction is calculated as shown in Figure 7, and the normal stress cloud diagram along the y -axis direction is shown in Figure 8.

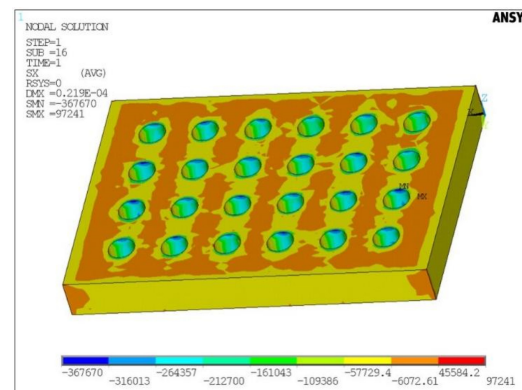


Figure 7. Normal stress cloud diagram along the x -axis.

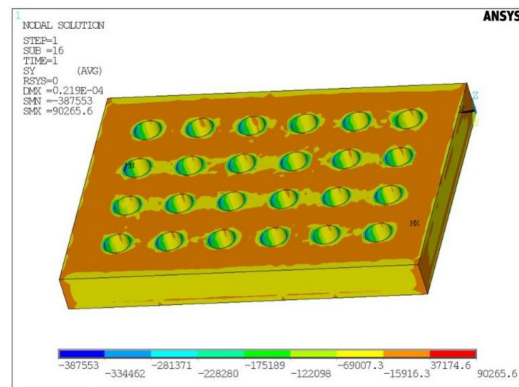


Figure 8. Normal stress cloud diagram along the y -axis.

From Figures 7 and 8, it can be seen that the maximum compressive stress of the bottom sealing concrete is 0.10 MPa, and the maximum tensile stress of the bottom sealing concrete is 0.39 MPa.

For the maximum bonding force of the bottom sealing concrete, it can be analyzed through the shear stress cloud diagram, as shown in Figures 9 and 10.

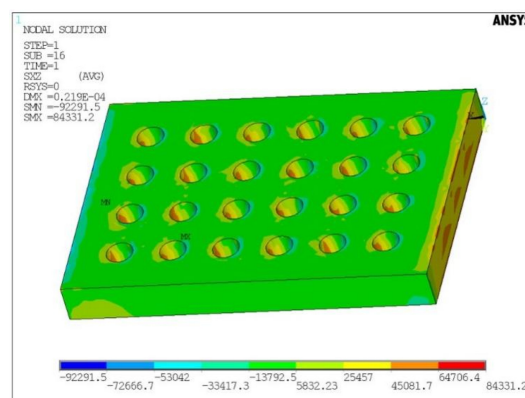


Figure 9. Shear stress cloud diagram along the z -axis on the x -axis normal plane.

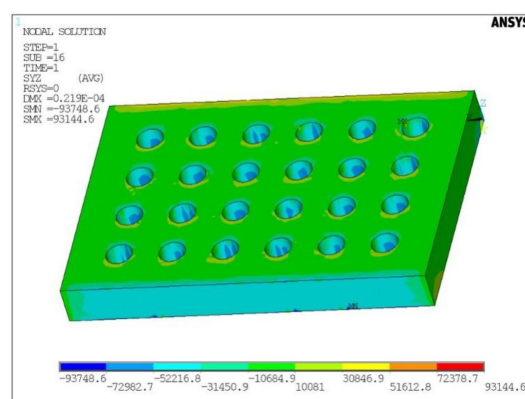


Figure 10. Shear stress cloud diagram along the z -axis on the y -axis normal plane.

It can be seen from Figures 9 and 10 that the maximum bonding force of the bottom sealing concrete is 93.75 kPa.

3.2. Theoretical Verification Calculation

3.2.1. Maximum Tensile Stress Verification Calculation

The approximate solution and the traditional method are used to calculate the maximum tensile stress of the bottom sealing concrete of the project, and then the monitoring

value of the maximum tensile stress of the bottom sealing concrete is calculated from the monitoring data of the project, and the maximum tensile stress obtained from the numerical simulation is compared, as shown in Table 2.

Table 2. Contrast of maximum tensile stress of bottom sealing concrete.

Data Sources	Maximum Tensile Stress/MPa	Relative Error Compared with Monitoring Data
Approximate Solution	0.95	2.96
Traditional Method	5.70	22.75
Numerical Simulation	0.39	0.625
Monitoring Data	0.24	0

Obviously, the maximum tensile stress calculated by the approximate solution is closer to the actual monitoring value than the traditional method.

3.2.2. Bonding Strength Verification Calculation

First use Equation (18) to calculate the average bonding force, and then compare it with the maximum bonding force obtained by numerical simulation, as shown in Table 3.

Table 3. Contrast of bonding force of bottom sealing concrete.

Data Sources	Bonding Force/kPa
Equation Calculation	89.61
Numerical Simulation	93.75

It can be seen that the average bonding force calculated using Equation (18) is slightly smaller than the numerical simulation value, and the error is about 4.62%.

4. Discussion

Regarding this paper, there are the following discussions:

- It can be seen that the tensile stress of the bottom sealing concrete calculated by the approximate solution is closer to the monitored value than the traditional method. Therefore, the approximate solution is more accurate than the traditional method.
- The result calculated by traditional method is safer in engineering. But, if the traditional method is adopted, the amount of concrete required during construction will be much larger, which will cause waste of materials.
- The numerical simulation method is closer to the monitored value than the above two theoretical calculation methods, but the steps are relatively cumbersome and require more time.
- When the accuracy required in the project is not high, the traditional method can be used; when the required accuracy is moderate, the approximate solution can be used; when the required accuracy is high, the numerical simulation method can be used.
- In the future research, for the elastic mechanics method, the influence of the holes in the bottom-sealed concrete can be considered to improve the accuracy of the calculation; for the numerical simulation method, the operation steps can be simplified.

5. Conclusions

Through the research of this paper, the following conclusions can be got that:

- When calculating the maximum compressive stress and tensile stress of the bottom sealing concrete, the concrete can be regarded as an isotropic, continuous, uniform, and small deformation elastic material, and the bottom sealing concrete can be simplified into an elastic thin slab, and the elasticity method is used for the calculation. The traditional method can also be used to divide the bottom sealing concrete slab

along the long side and divide it into several concrete beams. The maximum stress obtained by the approximate solution is closer to the actual monitoring value than the traditional method.

- Equation (18) can be used to calculate the ultimate bonding force between the bottom sealing concrete and the steel sleeves. The calculated bonding force is only an average value, and it will be slightly smaller, which can be used to make a rough estimate.
- For the calculation of the maximum compressive stress, tensile stress, and cohesive force of the bottom sealing concrete, it can be assumed that the bottom sealing concrete material is isotropic, homogeneous, and dense, and the ANSYS finite element software can be used for numerical simulation.

Author Contributions: Conceptualization, P.G. and Y.W.; methodology, S.C.; software, X.Z.; validation, P.G.; formal analysis, Y.L. (Yonghai Li) and Y.L. (Yan Liu); investigation, H.Y. All authors have read and agreed to the published version of the manuscript.

Funding: This research work was funded by the National Natural Science Foundation of China (42077249, 51774107), the Opening Project of State Key Laboratory of Explosion Science and Technology, Beijing Institute of Technology (KFJJ21-03Z), and the Fundamental Research Funds for Central Universities (JZ2021HGQA0247).

Institutional Review Board Statement: Not applicable.

Informed Consent Statement: Not applicable.

Data Availability Statement: All data, models, or codes that support the findings of this study are available from the corresponding authors upon reasonable request.

Conflicts of Interest: The authors declare that there are no conflict of interest regarding the publication of this paper.

References

1. Li, S.; Yao, A.; Ma, Y. Failure Mechanism and Passive Earth Pressure on Foundation Pits with Skirt Reinforcement. *Soil Mech. Found. Eng.* **2021**, *58*, 25–33. [\[CrossRef\]](#)
2. Wang, Z.; Zhang, N.; Li, Q.; Chen, X. Influence of Sand-Rubber Mixtures Backfill on Mechanical Properties of Bridge Abutment and Foundation Piles. *Soil Mech. Found. Eng.* **2018**, *55*, 55–61. [\[CrossRef\]](#)
3. Benmebarek, N.; Bensmaine, A.; Benmebarek, S.; Belouinar, L. Critical Hydraulic Head Loss Inducing Failure of a Cofferdam Embedded in Horizontal Sandy Ground. *Soil Mech. Found. Eng.* **2014**, *51*, 173–180. [\[CrossRef\]](#)
4. Blum, H. *Einspannung Sverhaeltnisse bei Bohlwerken*; Wilhelm Ernst & Sohn: Berlin, Germany, 1931.
5. Lohmeyer, E. Discussion to ‘Analysis of sheet pile bulkheads’ by P.Baumann. *Proc. Am. Soc. Civ. Eng.* **1934**, *61*, 347–355.
6. Terzaghi, K. Stability and stiffness of cellular cofferdams. *Am. Soc. Civ. Eng. Trans.* **1945**, *110*, 1083–1119. [\[CrossRef\]](#)
7. Ovesen, N.K. Cellular Cofferdams. Ph.D. Thesis, Danish Geotechnical Institute, Copenhagen, Denmark, 1962.
8. Banerjee, S.M. Design charts for double-walled cofferdam. *J. Geotech. Eng.* **1993**, *119*, 214–222. [\[CrossRef\]](#)
9. Clasmeier, H.D. A Comparison between Circular Cell Cofferdam and Double Wall Cofferdam. In Proceedings of the 11th International Harbour Congress, Antwerpen, Belgium, 17–21 June 1996.
10. Lefas, I.D.; Georgiannou, V.N. Analysis of a cofferdam support and design implications. *Comput. Struct.* **2001**, *79*, 2461–2469. [\[CrossRef\]](#)
11. Hu, Q. Study on the Application and Development of Double Wall Steel Cofferdam Technology for Bridge Foundation Construction. Master’s Thesis, Southwest Jiaotong University, Chengdu, China, 2005. (In Chinese)
12. Pan, H.; Wang, J.; Cao, H.; Luo, G. Research on Deformation and Internal Force Characteristics of Steel Sheet Pile Cofferdam under Different Construction Procedures. *Chin. J. Rock Mech. Eng.* **2013**, *32*, 2316–2324. (In Chinese)
13. Li, Y. Experiment of Sealing Properties and Structure Design for Steel Sheet Pile Cofferdam. Master’s Thesis, Central South University, Changsha, China, 2013. (In Chinese)
14. Wen, T. Model Test Study of Bonding Forces between Double-Wall Steel Cofferdam Base Sealing Concrete and Steel Pipe Pile. Master’s Thesis, Chongqing Jiaotong University, Chongqing, China, 2017. (In Chinese)
15. Chen, W. Study on the Anti-Floating Characteristics of the Concrete Bottom Sealing Structure of Deep Foundation Pit. Master’s Thesis, China University of Geosciences, Beijing, China, 2020. (In Chinese)
16. He, D. Study on the Construction Technology of the Steel Cofferdam in Complicated Hydro-Geological Conditions. Master’s Thesis, Chongqing Jiaotong University, Chongqing, China, 2016. (In Chinese)
17. Hua, H. Mechanical Behavior Analysis and Stress Monitoring of Double Wall Steel Cofferdam. Master’s Thesis, Chongqing Jiaotong University, Chongqing, China, 2017. (In Chinese)

18. Yu, J. Mechanical Characteristics Analysis and Key Technology Research of Single Wall Steel Cofferdam in Deep Water Construction. Master's Thesis, Changsha University of Science & Technology, Changsha, China, 2018. (In Chinese)
19. Divyah, N.; Thenmozhi, R.; Neelamegam, M. A comparative study on prediction models for strength properties of LWA concrete using artificial neural network. *Rev. Constr.* **2020**, *1523*, 103–111.
20. Alves de Souza, R.; Breña, S.F. Simplified nonlinear analysis of reinforced concrete coupling beams subjected to cyclic loading. *Rev. Constr.* **2020**, *13666*, 224–232. [[CrossRef](#)]
21. Shimpi, V.; Sivasubramanian, M.V.; Singh, S.B. Serviceability analysis and increased axle load performance of heritage arch gallery railway bridge. *Rev. Constr.* **2021**, *21471*, 178–189.
22. Guo, P.; Gong, X.; Wang, Y.; Lin, H.; Zhao, Y. Minimum cover depth estimation for underwater shield tunnels. *Tunn. Undergr. Space Technol.* **2021**, *115*, 104027. [[CrossRef](#)]
23. Guo, P.; Gong, X.; Wang, Y. Displacement and force analyses of braced structure of deep excavation considering unsymmetrical surcharge effect. *Comput. Geotech.* **2019**, *115*, 104027. [[CrossRef](#)]
24. Zhao, Y.; Wang, Y.; Wang, W.; Tang, L.; Liu, Q. Modeling of rheological fracture behavior of rock cracks subjected to hydraulic pressure and far field stresses. *Theor. Appl. Fract. Mech.* **2019**, *101*, 59–66. [[CrossRef](#)]
25. Zhao, Y.; Zhang, L.; Liao, J.; Wang, W.; Liu, Q.; Tang, L. Experimental Study of Fracture Toughness and Subcritical Crack Growth of Three Rocks under Different Environments. *Int. J. Geomech.* **2020**, *20*, 04020128. [[CrossRef](#)]
26. Zhao, Y.; Zhang, L.; Wang, W.; Liu, Q.; Tang, L.; Cheng, G. Experimental Study on Shear Behavior and a Revised Shear Strength Model for Infilled Rock Joints. *Int. J. Geomech.* **2020**, *2020*, 04020141. [[CrossRef](#)]
27. Wang, Y.; Zhang, H.; Lin, H.; Zhao, Y.; Liu, Y. Fracture behaviour of central-flawed rock plate under uniaxial compression. *Theor. Appl. Fract. Mech.* **2020**, *106*, 102503. [[CrossRef](#)]
28. Xu, Z. The Problem of Thin Slab Bending with Small Deflection and Its Classical Solution. In *Elasticity*, 5th ed.; CSPM: Beijing, China, 2016; Volume 2, pp. 20–23. (In Chinese)
29. Xu, Z. Thin Slab Bending Problem. In *A Concise Course in Elasticity*, 4th ed.; Higher Education Press: Beijing, China, 2013; pp. 215–217. (In Chinese)
30. Jin, G. Deep-Water Bridge Pile Foundation Steel Boxed Cofferdam Construction Technology Research. Master's Thesis, Chang'an University, Xi'an, China, 2011. (In Chinese)